

# Effect of triaxial stress-state on creep fracture in Inconel alloy X-750

M. C. PANDEY, A. K. MUKHERJEE

*Division of Materials Science and Engineering Department of Mechanical Engineering, University of California, Davis, California 95616, USA*

D. M. R. TAPLIN

*Department of Mechanical and Manufacturing Engineering, Trinity College, University of Dublin, Dublin-2, Ireland*

Smooth specimens and circumferentially notched bars with a "Bridgman" notch geometry were tested uniaxially at 700° C in air in the stress range of 340 to 700 MPa. The results indicated that the material was notch strengthened on the basis of net section stress,  $\sigma_a$ . However, when the fracture lifetimes were plotted as a function of the Bridgman effective stress,  $\sigma_e$ , all the data points fell approximately on one line. Cavity nucleation sites changed systematically from notch throat at the highest stress to notch root at the low stress. The notch rupture ductility in the notched specimens were found to have a lower value than in the smooth ones at all stresses.

## 1. Introduction

A component designed for high temperature units can be subjected to a complex stress system which may vary from uniaxial to triaxial stress-state. To make the most economical use of the component and to avoid premature failure, it is essential to study the effects of stress-state on creep deformation and fracture. The majority of the creep data have been obtained from the smooth specimens which are loaded uniaxially since it is convenient to perform the test in the laboratory. Design engineers being aware of this fact often used large safety factors in order to be on the conservative side. This often resulted in consistently larger section thickness in engineering design. The importance of this was realized and has been discussed in one of the papers at the fourth International Fracture Conference [1]. Multiaxial stress-state condition have been achieved using several techniques: (i) internally pressurized tubes with and without end loads [2]; (ii) torsional loading with and without uniaxial tension [3, 4]; (iii) cruciform type of specimens loaded under biaxial tension [5]; and (iv) circumferentially notched bar with a "Bridgman" notched geometry loaded uniaxially [6-8].

A considerable body of creep data for the notched specimens of low-alloy ferritic steels [9-12] and austenitic stainless steels [13] do exist but these investigations were mainly oriented towards the study of the effect of notch acuity and metallurgical factors on creep life. In view of the stress analysis done on the circumferentially notched bars with the Bridgman geometry [14, 15], it has now become possible to analyse the creep data of the specimens having such geometry (loaded uniaxially) in terms of the stress-state. The stress-state is found reasonably uniform over a large part of the notch throat. The present investigation reports the effect of triaxial stress-state (which is achieved in the circumferentially notched specimens loaded uniaxially) on cavitation and creep fracture lifetimes.

## 2. Experimental procedure

The material investigated is Inconel alloy X-750, a nickel-base superalloy. The nominal chemical composition of the material is as follows: 0.05 C, 6.51 Fe, 14.81 Cr, 2.68 Ti, 0.80 Al, 0.87 (Nb + Ta), 1.0 max Mn, 0.5 max Si, 0.01 max S and 73.2 Ni. Rectangular bars of size 12.5 mm × 12.5 mm were given standard industrial heat-treatment [16]:

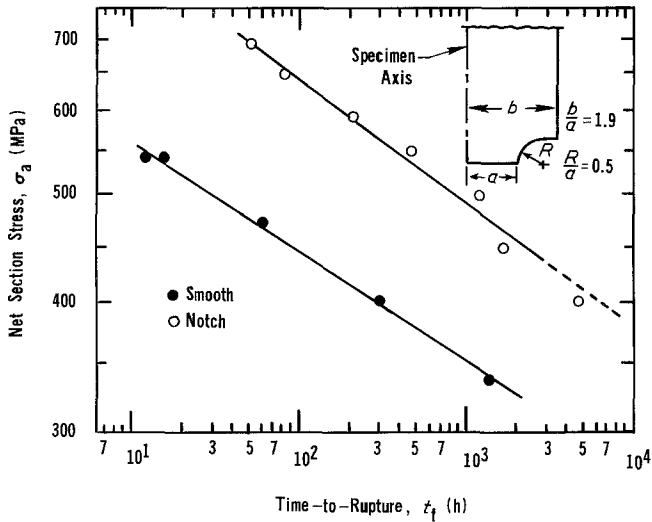


Figure 1 A plot of time-to-rupture against net section stress,  $\sigma_a$ , for smooth and circumferentially notched specimens. The material is notch strengthened on the basis of net section stress. Specimen geometry ( $b/a = 1.9$ ,  $r/a = 0.5$ ) is also shown.

1150°C for 4 h, air-cooled; 840°C for 24 h, air-cooled; and 710°C for 20 h, air-cooled. The heat-treatment resulted in a grain size of 160  $\mu\text{m}$ , measured by the linear intercept method. The heat-treatment bars were then machined to obtain smooth specimens (gauge diameter 5 mm and gauge length 25 mm) and notched specimens with two circumferential notches of 5 mm diameter each and 10 mm apart. The geometry of the notch is given in Fig. 1. The reason for using two notches was that if one notch failed, the other could be used for the metallographic examination to study the cavitation behaviour prior to fracture. The smooth and notched specimens were tested at 700°C in air in the stress range 340 to 700 MPa at constant load. The fractured and interrupted specimens were mid-sectioned and polished by conventional polishing techniques and then electroetched in a 5% nital solution.

### 3. Results and discussion

Using Bridgman's analysis [17], the effective stress,  $\sigma_e$ , has been calculated as follows:

$$\sigma_e = \sigma_a \left[ \left( 1 + \frac{2R}{a} \right) \ln \left( 1 + \frac{a}{2R} \right) \right]^{-1},$$

where  $\sigma_a$  is the net section stress and is equal to the load applied in uniaxial tension divided by the minimum cross-sectional area.  $\sigma_e$  is equal to 0.72 of the applied stress as calculated for the notch geometry under investigation. Hoop strain,  $\epsilon_H$ , is given by the expression:

$$\epsilon_H = \ln D_0/D,$$

where  $D_0$  and  $D$  are the initial and current diameters of plain bar and minimum notch sections.

A summary of the creep data of the smooth and notched specimens is given in Tables I and II.

TABLE I Creep fracture data of the notched specimens tested at 700°C in air

Net Section stress, $\sigma_a$ (MPa)	Bridgman effective stress, $\sigma_e$ (MPa)	Time-to-fracture (h)	Hoop strain to fracture $\epsilon_H = \ln D_0/D$ (%)
400	288	4628 (interrupted)	0.05
450	324	1312.5	5.20
500	360	1092	4.82
550	396	472	4.45
595	428	210	5.80
650	468	82.4	6.65
695	500	51	5.25

TABLE II Creep fracture data of the smooth specimens tested at 700° C in air

Stress (MPa)	$t_f$ (h)	Reduction of area (%)	$\epsilon_H$ $\epsilon_H = \ln D_0/D$ (%)
340	1330.5	17	9.30
400	305	20	11.20
472	60.5	23	13
540	15.5	12.30	6.6
540	12.5	12.02	6.40

Fig. 1 records the plot between net section stress,  $\sigma_a$ , and time-to-rupture,  $t_f$ , for both types of the specimens. The notched specimen subjected at 400 MPa was interrupted after 4625 h. After extrapolation of the curve, the time-to-rupture seems to be approximately 63 000 h. It can be noticed that the material is notch strengthened on the basis of net section stress. However, when the plot is made between Bridgman effective stress,  $\sigma_e$ , and time-to-rupture, as shown in Fig. 2, the creep data for both types of specimen geometry fall on one line (in uniaxial tension,  $\sigma_a = \sigma_e$ ). Thus, to a first approximation, the Bridgman effective stress,  $\sigma_e$ , predicts lifetimes reasonably well. Fig. 3 shows the plot between stress (both  $\sigma_a$  and  $\sigma_e$ ) and effective strain-to-fracture for both notched and smooth specimens. It shows that the effective strains at fracture in the notched specimens are lower than those in the smooth ones. The effective strain-to-fracture in the smooth specimens, first increases and then decreases with stress. In the notched specimens, the strain-to-fracture increases with stress and then it shows a tendency

to decrease. This becomes clearer when the fracture strain is compared on the basis of the effective stress (Fig. 3). The main reason for lower ductility at the highest stress seems to be environmental interactions during testing [18]. In a similar study to this, in Nimonic 80A [7], the effective strain-to-fracture was found to increase with stress. This seems to be due to the fine grain size (25  $\mu\text{m}$ ) and a different heat-treatment procedure employed for the Nimonic 80A.

A detailed metallography was performed to determine whether cavities first nucleated at the notch centre ( $r/a = 0$ ) or at the notch root ( $r/a = 1$ ). To check this, a notched specimen was tested at 695 MPa. The unfractured notch with hoop strain of 2.11% was examined for the cavity initiation site. Fig. 4 shows the size of cracks/cavities in the notch centre and adjacent to it. At the notch root, grain-boundary cracks of one grain facet in length were also observed. However, at 450 MPa, the unfractured notch with hoop strain of 1.12% revealed that there were no cracks/cavities at the notch centre, but a crack of one grain facet in length was observed at the distance of 0.75 mm from the notch root. The grain-boundary cracks of two grain facets were also observed at the notch root. In the interrupted notched specimen, tested at 400 MPa, only a crack of two grain facets was observed at the notch root. These findings clearly demonstrate that at the highest stress, the grain-boundary cavities nucleated at the notch centre, but with decrease in the stress, the fracture initiation site moved towards the notch root. It can be noticed that cavities/cracks always nucleated

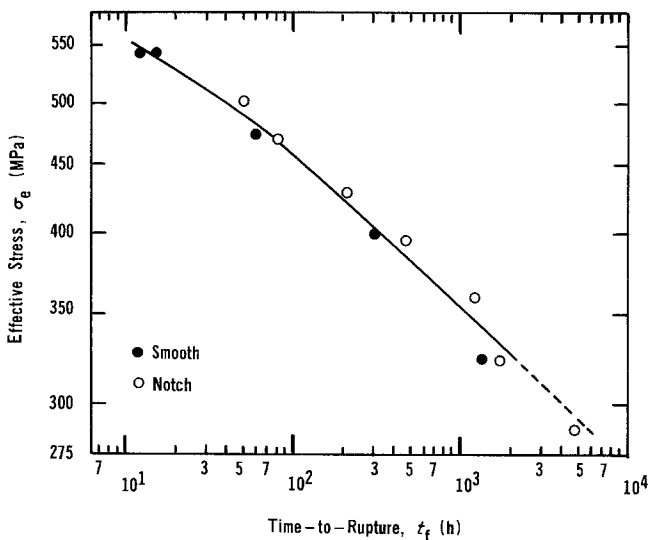


Figure 2 A plot of time-to-rupture against Bridgman effective stress,  $\sigma_e$ , showing that  $\sigma_e$  adequately represents the fracture lifetimes in the notched specimens.

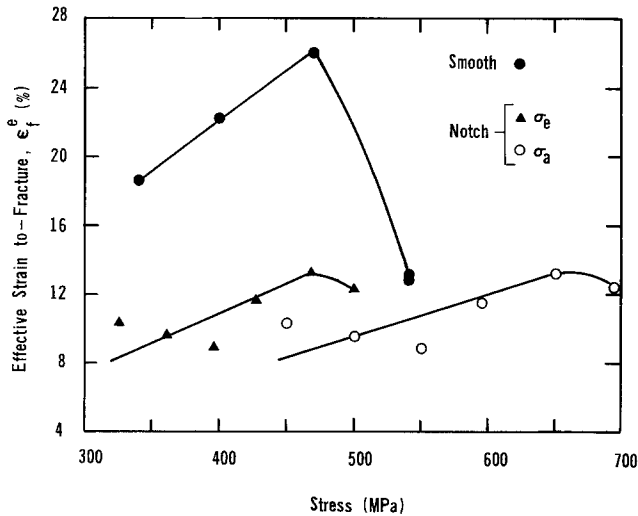


Figure 3 A plot of effective strain-to-fracture,  $\epsilon_e^f$ , ( $\epsilon_e^f = 2 \epsilon_H^f$ ) against stress (for both  $\sigma_e$  and  $\sigma_a$ ) showing that  $\epsilon_e^f$  for notched specimens is lower than that for uniaxial ones at all stresses.

at the notch root at all stresses. This was considered to be due to the grain-boundary cracks at the specimen's surface (Fig. 5). The grain-boundary cracks were observed in smooth specimens tested at both constant load and constant cross-head speed. However, the reason why the grain boundaries at the surface of the specimens crack is not understood, because the cracks were also observed in the vacuum-tested specimens [18]. It appears that oxygen diffuses along the cracked grain boundaries in the air-tested specimens causing a weakening effect. Fig. 6 depicts cavity/crack distribution in the specimen shown in Fig. 5. Fracture mode was intergranular at all stresses in both notched and smooth specimens (Figs. 7a to c).

Hayhurst and co-workers [14, 15] have shown that the maximum principal stress,  $\sigma_z$ , increases with increasing creep stress exponent,  $n$ , and the stationary state solutions are closely given by the

corresponding perfectly plastic solution for high values of  $n$ . In Inconel alloy X-750, the value of  $n$  is found to vary from 9 at 340 MPa to 20 at 600 MPa [20]. Fig. 8 shows the distribution of stress for  $n = 9$  for both the stationary state and plasticity solutions. It can be seen that  $\sigma_z$ , determined from both solutions are approximately the same, but  $\sigma_e$  values differ significantly. Previous results for this alloy [19] had shown that the time-to-rupture were controlled by both maximum principal stress and effective stress. Accordingly, the time-to-rupture in the notched specimens should have been controlled by both stresses. Instead, the Bridgman effective stress,  $\sigma_e$ , is found to control the rupture life. These results are similar to those obtained in Nimonic 80A. When uniaxial

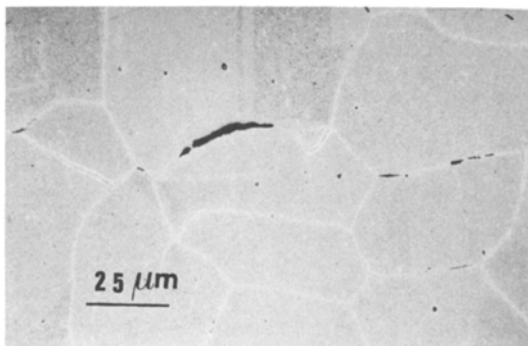


Figure 4 Single grain facet crack at the notch centre in the unfractured notch of the notched specimen tested at 695 MPa (hoop strain 2.1%).

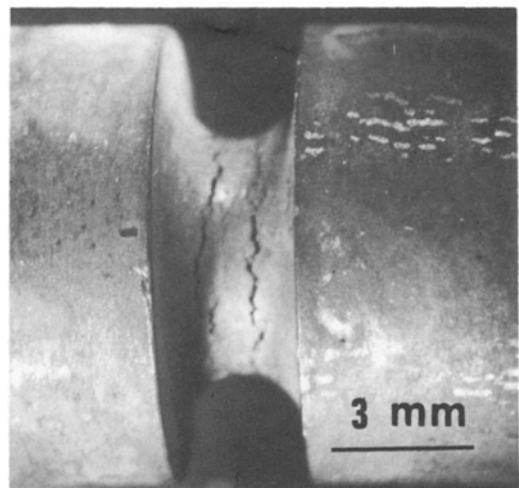
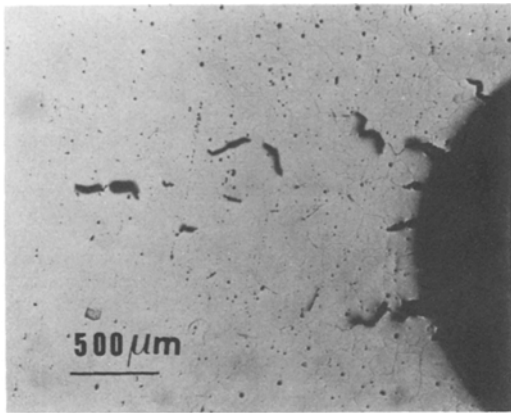


Figure 5 Grain-boundary cracks at the notch root of the interrupted specimen tested at 650 MPa.



*Figure 6* Cavity distribution from the notch root to the notch centre in the interrupted specimen tested at 650 MPa.

tension and torsion (biaxial) specimens were tested, the time-to-rupture was controlled by both maximum principal stress and effective stress [4] whereas in the notched specimens [7] it was controlled by the Bridgman effective stress. The value of  $n$  in Nimonic 80A was found to vary from 3 at low stress to 9 at high stresses. More creep data in specimens of different materials with Bridgman notch geometry are needed to determine the

rupture criterion. However, the results obtained in Inconel alloy X-750 and Nimonic 80A seem to indicate that irrespective of the value of  $n$ , the Bridgman effective stress adequately represents the rupture criterion for the notched specimens.

A study of the circumferentially notched test specimens has shown that notch-strengthening or notch weakening occurs depending on the uniaxial creep ductility and notch geometry [10]. It has generally been observed that the material with good uniaxial creep ductility and relatively shallow notches exhibits a pronounced strengthening effect. Although a material may show good uniaxial creep ductility, certain impurities segregated at the grain boundaries might become very sensitive to the stress-state, thereby causing nucleation of cavities and thus producing a notch-weakening effect. Since in the nickel-base alloys, grain-boundary cracking occurs at the specimen's surface, the presence of grain boundaries and its orientation should play a major role in deciding the fracture criterion and may sometimes lead to a large scatter in the creep data.

#### 4. Conclusions

The results obtained from the triaxial specimens with a Bridgman notch geometry loaded in uniaxial tension are:

1. The material is found to be notch strengthened on the basis of the net section stress;
2. Fracture lifetimes of components with a triaxial stress-state can reasonably be predicted using a rupture reference stress equal to the Bridgman effective stress;
3. The crack initiation site moved systemati-

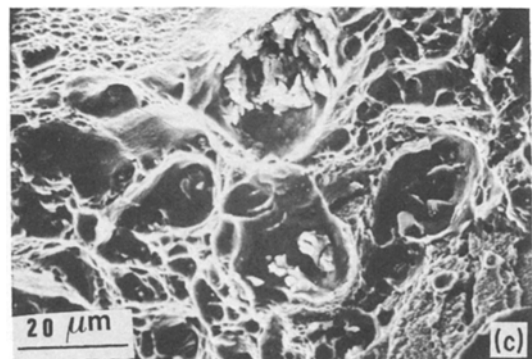
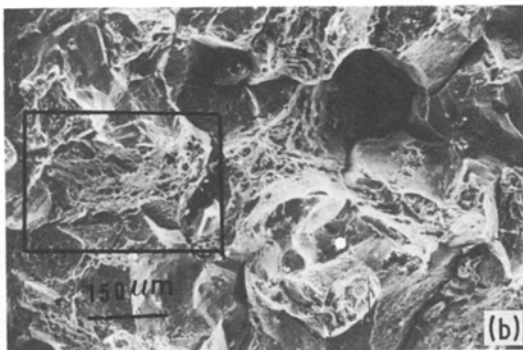
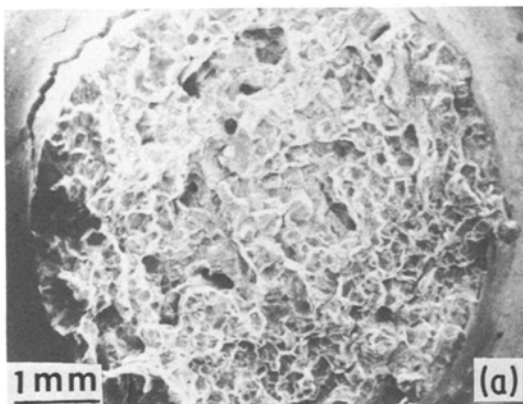


*Figure 7* Scanning electron fractographs of the notched specimen tested at a net section stress of 650 MPa at three different magnifications. Fractograph (c) is the enlarged view of the marked region in (b).

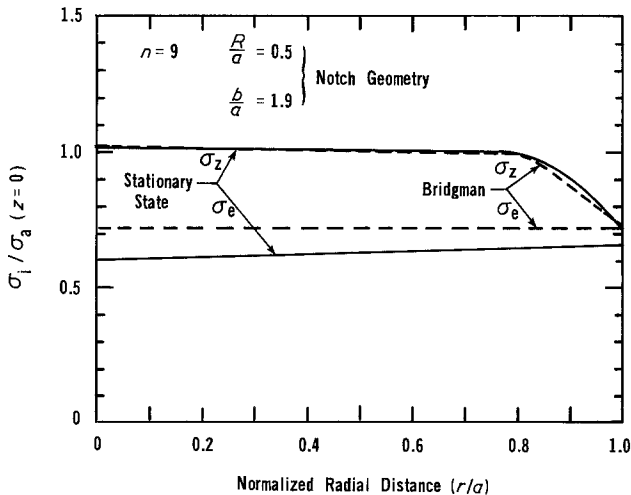


Figure 8 Spatial variation of stationary-state stresses obtained from finite element analysis (solid lines) and plasticity solutions (dotted lines), from notch centre ( $r/a = 0$ ) to notch root ( $r/a = 1$ ) for  $n = 9$ .

cally from notch centre at the highest stress towards the notch root at low stresses;

4. Fracture ductility in the specimens with the Bridgman notch geometry is lower than in the smooth specimens;

5. A cautious approach in using the reference stress concept for fracture criterion must be exercised since it may be different for the different stress-state.

### Acknowledgement

This work was supported by the Exxon corporation and the Department of Energy, Mines and Resources, Canada. One of the authors (MCP) wishes to acknowledge an NSF Post Doctoral Fellowship Award. The authors would like to express their gratitude to Dr B. F. Dyson for many stimulating discussions.

### References

1. D. MCLEAN, B. F. DYSON and D. M. R. TAPLIN, "The prediction of Creep Fracture in Engineering Alloys", The Fourth International Conference on Fracture, Vol. 1, edited by D. M. R. Taplin (University of Waterloo Press, Waterloo, Canada, 1977) pp. 325-62.
2. S. TAIRA and R. OHTANI, "Advances in Creep Design", edited by A. I. Smith and A. M. Nicholson, (Applied Science Publishers, London, 1971) p. 329.
3. A. E. JOHNSON, J. HENDERSON and B. KHAN, "Complex stress creep, Relaxation and Fracture of Metallic Alloys", (HMSO, Edinburgh, 1962).
4. B. F. DYSON and D. MCLEAN, *Metal Sci.* **11** (1977) 37.
5. D. KELLY, *Acta Metall.* **23** (1975) 1267.
6. M. S. LOVEDAY and B. F. DYSON, "Mechanical Behaviour of Materials", edited by K. J. Miller and R. F. Smith, ICM3, Vol. 2 (Pergamon, Oxford, 1980) pp. 213-22.
7. B. F. DYSON and M. S. LOVEDAY, Proceedings of IUTAM Conference on Creep Structures, Leicester, September (1980).
8. S. E. NG, G. A. WEBSTER and B. F. DYSON, "Notch Weakening and Strengthening in Creep of 1/2 Cr 1/2 Mo 1/4 steel." Advances in Fracture Research, ICF5, Canes, France, Vol. 3 (Pergamon, Oxford, 1981) pp. 1275-83.
9. W. F. BROWN, Jr, M. H. JONES and D. P. NEWMAN, Symposium on Strength and Ductility of Metals at Elevated Temperature with Particular References to Notches and Metallurgical Changes, ASTM STP 128 (1952) pp. 25-45.
10. E. A. DAVIS and J. J. MANJOINE, *ASTM STP* **128** (1952) 67.
11. R. M. GOLDHOFF and M. J. BEATTIE, Jr, *Trans. ASM* **57** (1964) 494.
12. R. M. GOLDHOFF and A. J. BROTHERS, *Trans. ASME J. Basic Engineering* **90** (1968) 37.
13. F. GARAFALO, *ASTM* **59** (1959) 957.
14. D. R. HAYHURST, F. A. LECKIE and J. T. HENDERSON, *Int. J. Mech. Sci.* **19** (1977) 147.
15. D. R. HAYHURST and J. T. HENDERSON, *Int. J. Mech. Sci.* **19** (1977) 133.
16. Inconel alloy X-750, Huntinton Alloys, The International Nickel Company, Inc., West Virginia (1963).
17. P. W. BRIDGMAN, "Large Plastic Flow and Fracture", (McGraw Hill, New York, 1952).
18. M. C. PANDEY, D. M. R. TAPLIN and A. K. MUKHERJEE, *Met. Trans.* **15A** (1984) 1763.
19. M. C. PANDEY, B. F. DYSON and D. M. R. TAPLIN, *Proc. Roy Soc. A* **393** (1984) 117.
20. M. C. PANDEY, Ph D thesis, University of Waterloo, Canada (1982).

Received 13 April  
and accepted 10 May 1984